Non-GMO potato lines, synthesizing increased amylose and resistant starch, are mainly deficient in isoamylase debranching enzyme

Blennow, Andreas; Skryhan, Katsiaryna; Tanackovic, Vanja; Krunic, Susanne L.; Shaik, Shahnoor Sultana; Andersen, Mette S.; Kirk, Hanne Grethe; Nielsen, Kåre Lehmann

Published in:
Plant Biotechnology Journal

DOI (link to publication from Publisher):
10.1111/pbi.13367

Publication date:
2020

Document Version
Publisher's PDF, also known as Version of record

Plant Biotechnology Journal
Open Access

Plant Biotechnology Journal (2020) **18**, pp. 2096–2108 doi: 10.1111/pbi.13367

Non-GMO potato lines, synthesizing increased amylose and resistant starch, are mainly deficient in isoamylase debranching enzyme

Andreas Blennow[1,*], Katsiaryna Skryhan[1], Vanja Tanackovic[1], Susanne L. Krunic[1], Shahnoor S. Shaik[1], Mette S. Andersen[2], Hanne-Grethe Kirk[3] and Kåre L. Nielsen[2]

[1]*Department of Plant and Environmental Sciences, University of Copenhagen, Frederiksberg C, Denmark*
[2]*Department of Chemistry and Biology, Aalborg University, Aalborg, Denmark*
[3]*Danish Potato Breeding Foundation, Vandel, Denmark*

Received 4 November 2019;
revised 31 January 2020;
accepted 17 February 2020.
**Correspondence* (Tel +45 35333304; fax +45 35333333; email abl@plen.ku.dk)

Keywords: starch, *Solanum tuberosum*, *Solanum sandemanii*, introgression, genome sequencing, transcript analysis, polysaccharides, bioengineering, non-GM crops.

Summary

Solanum tuberosum potato lines with high amylose content were generated by crossing with the wild potato species *Solanum sandemanii followed by repeated backcrossing to Solanum tuberosum lines.* The trait, termed increased amylose (IAm), was recessive and present after three generations of backcrossing into *S. tuberosum* lines (6.25% *S. sandemanii* genes). The tubers of these lines were small, elongated and irregular with small and misshaped starch granules and high sugar content. Additional backcrossing resulted in less irregular tuber morphology, increased starch content (4.3%–9.5%) and increased amylose content (29%–37.9%) but indifferent sugar content. The amylose in the IAm starch granules was mainly located in peripheral spots, and large cavities were found in the granules. Starch pasting was suppressed, and the digestion-resistant starch (RS) content was increased. Comprehensive microarray polymer profiling (CoMPP) analysis revealed specific alterations of major pectic and glycoprotein cell wall components. This complex phenotype led us to search for candidate IAm genes exploiting its recessive trait. Hence, we sequenced genomic DNA of a pool of IAm lines, identified SNPs genome wide against the draft genome sequence of potato and searched for regions of decreased heterozygosity. Three regions, located on chromosomes 3, 7 and 10, respectively, displayed markedly less heterozygosity than average. The only credible starch metabolism-related gene found in these regions encoded the isoamylase-type debranching enzyme Stisa1. Decreased expression of mRNA (>500 fold) and reduced enzyme activity (virtually absent from IAm lines) supported *Stisa1* as a candidate gene for IAm.

Introduction

Resistant and high-amylose starch

Starch can be considered as the most important multipurpose polysaccharide product worldwide with an annual global production in 2011 amounting 73 million tons (Giract Organization, 2011), which is projected to reach 150 million tons by 2024 (Global Industry Analysts). The European Union produces 1.2 million tons of starch from potato. The balance between the two main molecular fractions of starch, normally constituting an amylose of 20%–30% and an amylopectin of 70%–80%, is important for starch functionality and nutritional value. Amylose is only slightly branched by α-1,6 linkages while amylopectin is approximately 5% branched by clustered branch linkages (Damager *et al.*, 2010; Perez and Bertoft, 2010). Normally, starch intake induces postprandial high blood glucose and insulin responses (Swallow, 2003) and overconsumption of starch-rich foods leads to lifestyle-related diseases including obesity and diabetes. However, resistant starch (RS) (Englyst *et al.*, 1992) can escape degradation in the upper gut and can reduce appetite and prevent obesity by ileal and/or colonic brake (Lee *et al.*, 2013). Subsequent fermentation of RS in the colon by gut microbiota releases short-chain fatty acids (SCFAs) including butyrate, which are efficiently metabolized by colonocytes (Lee *et al.*, 2013) and have demonstrated health benefits (Bird *et al.*, 2000). Amylose is positively correlated with RS and reduced glycaemic responses (Regina *et al.*, 2006), and its amylolytic resistance is a direct result of the repetitive amylose backbone structure that can form insoluble and crystalline aggregates (Htoon *et al.*, 2009; Shrestha *et al.*, 2010).

High-amylose crops

A number of starch crops, especially cereals, have been bred and modified to synthesize high-amylose starch (Blennow *et al.*, 2013; Carciofi *et al.*, 2011; Regina *et al.*, 2012; Sestili *et al.*, 2010). The typical strategy is to suppress starch branching enzyme (SBE) or starch synthase (SS), reducing the biosynthesis of amylopectin resulting in high amylose and often long-chain amylopectin. To this end, an amylose-only (99%) starch was generated by suppressing all three SBEs in the barley grain (Carciofi *et al.*, 2011). Potato tuber starch has relatively low amylose content, approximately 20%, it is easily digested by amylase and therefore confers high postprandial glycaemic loads Fernandes *et al.*, 2005). Breeding potato cultivars to synthesize high-amylose starch is attractive from a nutritional point of view, but the tetraploid nature of elite potato

(Uitdewilligen *et al.*, 2013) complements possible mutations that confer the recessive high-amylose trait (loss of gene function) resulting in low natural variation in amylose content. As an alternative, transgenic approaches using antisense and RNA interference (RNAi) suppression of SBE activity in the tuber have generated high-amylose potato lines (Blennow *et al.*, 2005; Hofvander *et al.*, 2004; Schwall *et al.*, 2000). The starch granules of these lines are highly distorted and amylose contents up to 78% have been documented (Hofvander *et al.* 2004). An important side effect that is prominent in potato is the increase in the level of starch phosphate in these lines resulting in increased hydration (Blennow *et al.*, 2005; Hofvander *et al.*, 2004; Schwall *et al.*, 2000). The amylolytic degradability of such starch types is altered (Wickramasinghe *et al.*, 2009) although it is not always directly correlated to the content of amylose and additional factors such as microstructure can be important.

Biotechnologies for starch bioengineering

RNAi technology most often involves the transfer of foreign genes to the crop generating so-called GM (genetically modified) crops. Public concern about the use of these crops has stimulated the development of alternative methods for generating new starch qualities, including high amylose, in crops. Alternatively, the use of so-called cisgenesis (Schouten and Jacobsen, 2008), uses endogenous genes or genes from closely related species, has been considered. Random mutagenesis is generally regarded as safe and non-GM, and in the case of starch bioengineered for high amylose content, advanced mutant induction and screening including targeting induced local lesions (TILLING) in genomes of wheat (Hazard *et al.*, 2012; Slade *et al.*, 2012) and simple sequence repeat (SSR) markers in BEIII in rice (Yang *et al.*, 2012) has been introduced as non-GM strategies to isolate natural high-amylose lines. So far, no attempts to use mutagenesis combined with advanced screening for high-amylose potato have been documented. However, the discovery of a low-glycaemic index potato cultivar (Ek *et al.*, 2014) adds important contribution to low glycaemic potatoes based on RS. Interestingly, no correlation to amylose content was found for this potato cultivar suggesting additional molecular factors being responsible for the reduced digestibility of the starch. Precise genome editing (PGE) has been introduced for starch bioengineering targeting specific genes by mutagenesis, generating non-GM crops. Recently the CRISPR/Cas9 (clustered regularly interspaced short palindromic repeats/Cas9) system was used to knock out the granule-bound starch synthase (GBSS) to generate amylose-free potato tuber starch (Clasen *et al.*, 2015; Johansen *et al*, 2019; Veillet *et al.*, 2019) and combinations of SBEI and SBEII to achieve high-amylose potato starch (Tuncel *et al.*, 2019).

Metabolic steps affecting amylopectin branching and amylose content

Isoamylase (ISA) isoforms ISA1 and ISA2 have been demonstrated to have major effect on starch biosynthesis by facilitating the crystallization of highly branched pre-amylopectin to influence the final semi-crystalline structure of amylopectin (Hennen-Bierwagen *et al.*, 2012; Streb and Zeeman, 2014). ISAs are conserved in many plant species and knocking out or knocking down ISA activity in plants typically results in the formation of phytoglycogen at the expense of starch, including amylose (Streb and Zeeman, 2014). Potato harbours three specific isoamylase isoforms termed Stisa1, Stisa2 and Stisa3, and their expression suggests their involvement in starch biosynthesis. Stisa1 and Stisa2 are associated in a heteromeric enzyme complex and thought to be directly involved in starch biosynthesis (Hussain *et al.*, 2002). However, Stisa2 does not seem to have hydrolytic activity but might have a regulatory role (Hussain *et al.*, 2002). Parallel to potato, the Arabidopsis ISA1 requires ISA2 as a partner in a complex (Facon *et al.*, 2013). In maize, either homomeric or heteromeric ISA can be involved in starch biosynthesis (Kubo *et al.*, 2010) and maize Isa1 alone can support starch biosynthesis when expressed in Arabidopsis (Facon *et al.*, 2013). In rice, like in maize, ISA1 only forms a homo-oligomer complex and this is essential for starch biosynthesis (Utsumi *et al.*, 2011). Interestingly, in potato, ISA has been suggested to be also involved in the control of initiation of starch granule formation. Based on that, RNAi targeted transgenic potato tubers were generated, which had reduced expression of Stisa1 or Stisa2 and accumulates soluble and highly branched so-called phytoglycogen and a large numbers of small starch granules (Bustos *et al.*, 2004). In rice, QTL analysis of grain chalkiness and RNAi suppression of *ISA1* indicates that ISA expression increases grain chalkiness (Wenqian *et al.*, 2016).

We recently documented an AFLP fragment derived from the wild species *S. sandemanii* that is associated with altered starch deposition in the potato tuber (Krunic *et al.*, 2017). The absence of the sequence was shown to result in increased amylose in the tuber starch and was termed IAm, for **i**ncreased amylose. The recessive IAm trait was transferred to modern tetraploid *S. tuberosum* potato cultivars together with 6.25% of *S. sandemanii* genes in backcross 3 (BC3) lines. Increased starch granule-bound Pho1 activity and decreased SS activity was suggested to contribute to the phenotype characteristic of having small starch granules since Pho1 is suggested to be involved in the granule initiation (Nakamura *et al.*, 2012). However, the increased amylose was not readily explained. In the present study, we provide genomic, transcriptomic and enzymatic activity evidence that the IAm trait in BC4 potato lines is caused by absence of Stisa1 activity but likely also requires additional factors such as previously identified increased granule-associated Pho1 activity and decreased SS protein.

Results

Tuber yield and morphology

Field trials resulted in yields for the BC4 IAm lines in the range 0.29–0.85 kg/plant. This was considerably less and more variable than the control cultivars with yields ranging 1.22–1.56 kg tubers/plant (Table S2). Line 12-727-6 had the most severe (elongated and misshaped) tuber phenotype (Figure S1) and lowest yield. However, apart from this line, no general relationship was found between tuber morphology and tuber yield. The BC4 IAm tubers in this investigation having a calculated 3.125% of *S. sandemanii* DNA were more similar to control than BC3 lines having 6.25% *S. sandemanii* genes. The above-ground phenotype was not significantly different from the tuberosum controls (not shown), and again, this was different from the BC3 lines which displayed severe phenotypes with e.g. multiple above-ground stolons and stems (Krunic *et al.*, 2017).

Tuber starch and sugar content

The starch content in the BC4 lines—IAm tubers was low and ranged 4.3%–9.5% fresh weight (FW) as compared to the control tubers which ranged 19.1%–20.5% (Table 1). The BC3 lines had lower starch content ranging 2.5%–5.6% (Krunic *et al.*,

2017). Sugars in the BC4 IAm lines were rather high, 4.9%–14.7%, and indifferent from the BC3 lines (5.5%–13.0%, Krunic *et al.*, 2017) compared with 1.8%–5.8% FW for the control lines. Hence, reduction in the *S. sandemanii* gene content in the IAm tubers from BC3 to BC4 substantially increased starch content. We found no detectable amounts of maltooligosaccharides or higher Mw glucans (less that 50 μg/g FW, including phytoglycogen, in all the samples following an extraction protocol with water instead of 80% ethanol.

Apparent amylose, amylopectin chain-length distribution and starch phosphate content

The apparent amylose content, as determined by iodide complexation (Table 1), documents the increased amylose content (29.0%–37.9%) as compared to control lines (19.8%–21.0%), also showed that the IAm lines in the BC4 collection were slightly higher as compared to the BC3 lines (26.3%–32.7%; Krunic *et al.*, 2017). The chain-length distribution of amylopectin, as investigated by HPAEC-PAD, confirmed the previous data on BC3 potato lines homozygous for the IAm locus (Krunic *et al.*, 2017) demonstrating a minor specific change in the chain-length profile (not shown). However, no significant reduction in the average chain length could be detected for the BC4 lines; the controls were in the range DP 31.9–32.8 and IAm lines ranged DP 27.8–38.4. However, the content of phosphate esterified at the C-3 and C-6 position of the IAm starch was significantly increased from the control range 5.7–7.6 nmol/mg starch for Glc3P and 11.9–20.3 for Glc6P ranged 6.3–9.8 for Glc3P and 25.0–37.7 for Glc6P. Hence, the increase was mainly attributed to the content of Glc6P which we previously associated to an increase in the soluble glucan water dikinase 1 protein (Krunic *et al.*, 2017) catalysing phosphorylation at the 6-position of the glucose residues.

Table 1 Starch content and main starch chemical characteristics of the starch in the IAm lines of BC4

Sample	Starch (% FW)	Amylose (%)	Mean CL (DP)	Glc3P nmol/mg starch	Glc6P nmol/mg starch
STABILO	20.5 ± 0.9	21.0 ± 0.1	32.3	7.4 ± 0.8	16.0 ± 0.9
KATINKA	19.0 ± 0.5	18.0 ± 2.0	31.9	6.2 ± 1.9	14.2 ± 0.7
93-CAL-3	19.1 ± 1.3	20.8 ± 2.8	32.6	7.6 ± 0.8	20.3 ± 0.8
94-BVB-6	19.8 ± 1.4	19.8 ± 0.0	32.8	5.7 ± 0.4	11.9 ± 0.3
12-702-2	8.4 ± 1.8	33.5 ± 0.2	32.2	8.2 ± 1.2	28.9 ± 1.1
12-702-3	9.1 ± 1.0	33.8 ± 0.7	31.8	6.3 ± 0.7	25.9 ± 0.8
12-712-8	nd	nd	nd	nd	nd
12-702-6	9.5 ± 0.6	33.2 ± 0.7	27.8	7.2 ± 0.8	26.8 ± 2.4
12-712-8	6.5 ± 1.7	33.8 ± 0.7	35.9	7.8 ± 0.8	30.3 ± 0.8
12-713-3	7.2 ± 0.9	37.2 ± 1.3	32.5	8.1 ± 0.4	26.3 ± 1.2
12-713-7	9.8 ± 0.2	37.9 ± 1.1	38.4	7.0 ± 1.4	25.6 ± 0.8
12-715-5	5.5 ± 1.3	32.6 ± 0.5	30.0	8.0 ± 0.1	26.4 ± 0.3
12-716-1	4.3 ± 1.0	30.1 ± 0.7	31.5	7.5 ± 0.8	25.0 ± 0.6
12-723-1	5.8 ± 0.9	34.8 ± 0.0	31.0	7.3 ± 0.3	30.6 ± 0.8
12-727-6	7.0 ± 1.2	36.0 ± 0.2	32.4	8.1 ± 1.2	29.5 ± 0.6
12-739-4	5.9 ± 0.8	29.0 ± 0.6	32.8	9.8 ± 0.4	37.7 ± 1.7

Mean CL: mean degree of polymerization (DP) chain-length distribution of amylopectin, Glc3P and Glc6P: the content of phosphate esters at the C-3 and C-6 position of the starch.

Starch granule size distribution and microstructure

The starch granules of the IAm lines were smaller and all size parameters including volume distribution mean diameter (MV), number distribution (MN) and area distribution (MA) were almost half for the IAm lines as for the control lines, for example the MV was on average 27.1 for the IAm lines and 47.1 for the controls (Table 3). Microscopic analysis of the starch granules revealed several unique features. As compared to the normal control granule (Figure 1a,b), confocal microscopy using Safranin O as fluorophore, many IAm starch granules showed hollow and irregular structures (Figure 1c,e) and starch granules with a sheath-like morphology were also evident (Figure 1e,f). Using APTS as a probe for the reducing end of the starch molecules, thereby mainly staining amylose, revealed a clustered distribution of amylose (Figure 1g,i). Typically, the regions enriched in amylose were located in spots at the periphery of the starch granules (Figure 1g) or along the periphery (Figure 1i). Scanning electron microscopy (SEM) revealed surface characteristics that were highly irregular and rough (Figure 2). In the high-amylose line 12-723-1, we identified multiple granule initiations (Figure 2a) and in line 12-713-7 highly disorganized granule surfaces (Figure 2b). In line 12-739-4 and control, representing low amylose content, more normal starch granules were observed (Figure 2c,d).

Pasting properties

The pasting characteristics displayed severe reductions in viscosity. Peak viscosity (PV) was more than fivefold lower; hot paste viscosity (HPV) more than threefold lower; breakdown (BD) more than 260-fold lower; and final viscosity (FV) more than 10-fold lower than controls. The setback (SB) parameter displayed great variation and the peak temperature (PT) was typically increased (Table 4). The data are generally in agreement with potato starch having increased amylose resulting in restricted swelling and increased gel-forming capacity (Blennow *et al.*, 2005; Wickramasinghe *et al.*, 2009). However, we expected to observe higher SB values for these starches as an effect of the increased amylose providing higher gel-forming tendency than typical potato starch.

In vitro enzymatic starch hydrolysis

The resistant starch (RS) content for the gelatinized samples was somewhat higher for the IAm lines (69 ± 3%) as for the control starch (63 ± 4%). The difference in RS between control and IAm starch (6%) was is in the same range as for the lines with higher *S. sandemanii* gene content (8%) (Krunic *et al.*, 2017). Hence, the RS was at levels as expected for the moderately increased amylose found in the IAm lines.

Comprehensive microarray polymer profiling (CoMPP) analysis

The altered tuber phenotype especially for line 12-727-6 (Figure S1) indicates a disturbance of the cell wall biosynthesis in the tubers. CoMPP analysis of the major expected cell wall polysaccharides revealed specific alterations of the cell wall components of the tubers (Figure 3). First, none of the mutants had increased levels of any of the polysaccharides. However, some polysaccharides were more abundant in the IAm lines than in the control lines. These components include the pectic components arabinan (detected by the mAb LM13 and the mAb LM6 antibodies), rhamnogalacturonan I backbone (detected by the mAb INRA-RU2 and mAb INRA-RU1 antibodies) and the homogalacturonan (detected by the mAb

Table 2 Sugar profiling

Sample	Trehalose	Arabinose	Glucose	Fructose	Sucrose	Maltose	Total
Stabilo	0.4 ± 0.2	0.0 ± 0.0	2.7 ± 0.9	1.3 ± 0.1	1.1 ± 0.1	0.3 ± 0.1	5.8 ± 1.1
Katinka	0.3 ± 0.2	0.2 ± 0.0	0.3 ± 0.1	0.1 ± 0.0	3.5 ± 1.5	0.4 ± 0.0	4.8 ± 1.7
93-CAL-3	0.2 ± 0.1	0.2 ± 0.1	1.0 ± 0.4	0.2 ± 0.0	3.3 ± 1.4	0.3 ± 0.0	5.1 ± 1.8
94-BVB-6	0.2 ± 0.1	0.0 ± 0.1	0.6 ± 0.2	0.1 ± 0.0	0.4 ± 0.3	0.3 ± 0.1	1.8 ± 0.7
Oleva	0.2 ± 0.1	0.0 ± 0.0	0.5 ± 0.2	0.1 ± 0.0	1.0 ± 0.3	0.3 ± 0.1	2.1 ± 0.6
12-702-2	0.5 ± 0.1	0.3 ± 0.0	0.4 ± 0.1	0.2 ± 0.0	8.5 ± 1.1	0.5 ± 0.1	10.3 ± 1.1
12-702-3	0.3 ± 0.1	0.2 ± 0.0	0.8 ± 0.2	0.2 ± 0.0	4.7 ± 1.3	0.3 ± 0.0	6.5 ± 1.6
12-702-8	1.6 ± 0.6	0.4 ± 0.0	0.2 ± 0.1	0.2 ± 0.0	11.6 ± 2.7	0.5 ± 0.1	14.7 ± 2.8
12-712-6	0.3 ± 0.2	0.3 ± 0.1	0.7 ± 0.2	0.8 ± 0.2	3.9 ± 1.3	0.3 ± 0.0	6.3 ± 2.0
12-712-8	0.6 ± 0.4	0.0 ± 0.0	1.4 ± 0.7	0.4 ± 0.0	3.7 ± 1.4	0.6 ± 0.2	6.7 ± 2.3
12-713-3	0.2 ± 0.1	0.1 ± 0.0	1.1 ± 0.2	0.2 ± 0.0	6.9 ± 0.8	0.3 ± 0.0	8.9 ± 1.0
12-713-7	0.2 ± 0.1	0.1 ± 0.0	0.4 ± 0.1	0.2 ± 0.1	8.7 ± 0.6	0.3 ± 0.1	9.8 ± 0.6
12-715-5	0.2 ± 0.1	0.2 ± 0.0	1.5 ± 0.3	0.2 ± 0.1	6.4 ± 1.0	0.4 ± 0.1	9.0 ± 1.1
12-716-1	0.2 ± 0.1	0.0 ± 0.0	2.9 ± 0.4	0.2 ± 0.0	1.3 ± 0.3	0.3 ± 0.0	4.9 ± 0.7
12-723-1	0.3 ± 0.1	0.0 ± 0.0	7.9 ± 0.9	0.0 ± 0.0	7.9 ± 1.5	0.4 ± 0.0	16.6 ± 1.7
12-727-6	0.2 ± 0.1	0.0 ± 0.0	2.3 ± 0.2	0.4 ± 0.1	8.1 ± 1.6	0.3 ± 0.0	11.4 ± 1.9
12-739-4	0.4 ± 0.3	0.2 ± 0.0	1.0 ± 0.5	0.4 ± 0.1	8.5 ± 1.5	0.4 ± 0.1	10.9 ± 2.2

Concentration in mg/mg fresh weight.

Table 3 Starch granule size distribution based on volume distribution mean diameter (MV), number distribution (MN), area distribution (MA) and graphic standard deviation (SD), nd: not determined

Line	MV	MN	MA	SD
Stabilo	49.3	33.2	43.5	14.3
Katinka	46.0	27.1	39.5	15.5
93-CAL-3	43.6	23.1	36.2	16.0
94-BVB-6	49.6	28.3	42.6	15.7
Oleva	nd	nd	nd	nd
12-702-2	27.0	16.9	23.3	9.4
12-702-3	25.7	14.6	21.1	9.2
12-702-8	23.0	12.5	19.2	8.5
12-712-6	nd	nd	nd	nd
12-712-8	27.4	13.9	21.6	11.7
12-713-3	26.4	14.1	21.0	10.7
12-713-7	31.7	14.6	23.7	14.7
12-715-5	31.7	14.6	23.7	14.7
12-716-1	26.1	12.0	19.8	12.3
12-723-1	26.1	12.0	19.8	12.3
12-727-6	27.7	14.4	21.9	11.7
12-739-4	32.5	16.7	24.8	14.3
Average Controls	47.1	27.9	40.4	15.4
Average IAm	27.7	14.2	21.8	11.8

2F4 and mAb LM19 antibodies). Among the components that were also increased were the glycoproteins extensin (detected by the mAb LM1, mAb JIM11and mAb JIM20 antibodies) and the arabinogalactan gum (AGP) (detected by the mAb JIM13 antibody). The control line Stabilo was an outlier among the control lines and had cell wall composition comparable to the IAm lines. Interestingly, the NaOH soluble (1 → 3)-β-D-glucan (the mAb BS-400-2 antibody), abundant in cereals, was detected in the mutants but not in the controls. Again, control cultivar Stabilo was an outlier containing (1 → 3)-β-D-glucan at the same level as the IAm lines.

Three genomic regions have low heterozygosity in the pool of IAm lines

The IAm trait appears recessive from the crossing statistics (data not shown). However, we cannot completely rule out that a 3:1 ratio of loss of function:normal function at the causal loci can lead to increased amylose content due to haplotype insufficiency. Nonetheless, all lines must be homozygous (or near-homozygous) for the DNA fragment(s) from *S. sandemanii* encoding the gene(s) to fully express the phenotype. Following genomic DNA sequence read mapping and variant calling of the pool of 15 potato lines, the ratio of heterozygous SNPs and total SNPs (both homo- and heterozygously different from the genome model) were calculated in 1 Mb bins across the genome sequence (Figure 4). Three relatively large regions on chromosome 3 (5–30 Mb), chromosome 7 (5–40 Mb) and chromosome 10 (10–21 Mb) showed markedly less heterozygosity than average and is thus likely to contain gene (s) responsible for the IAm phenotype. Using the starch metabolism gene list from Schreiber *et al.* (2014), no starch metabolism-related genes were found on the region of chromosomes 3 and 10 (except an invertase (PGSC0003DMG400020699), which is annotated as a likely pseudogene by Schreiber *et al.,* 2014) and only two genes were found in the region on chromosome 7, namely debranching enzyme isoamylase isoform 1 DBE-7 (PGSC0003DMG400020699) and ADP-glucose pyrophosphorylase large subunit AGPaseS-7 (PGSC0003DMG400015952).

Isoamylase 1 is the most differentially expressed gene in the high-amylose lines

The gene expression of the group of the IAm lines was compared to the group of cultivars used for backcrossing by RNA-Seq (Figure 4). Out of 39028 detected transcripts, 186 were differentially expressed between the two groups (FDR corrected *P*-value < 0.05; Table S3). Of these, only two genes encoding isoamylases were found in the starch metabolism-related gene list (Schreiber *et al.*, 2014). Strikingly, the gene that exhibits the highest fold change between the IAm and control was debranching enzyme isoamylase isoform 1 DBE-7 (PGSC0003DMG400

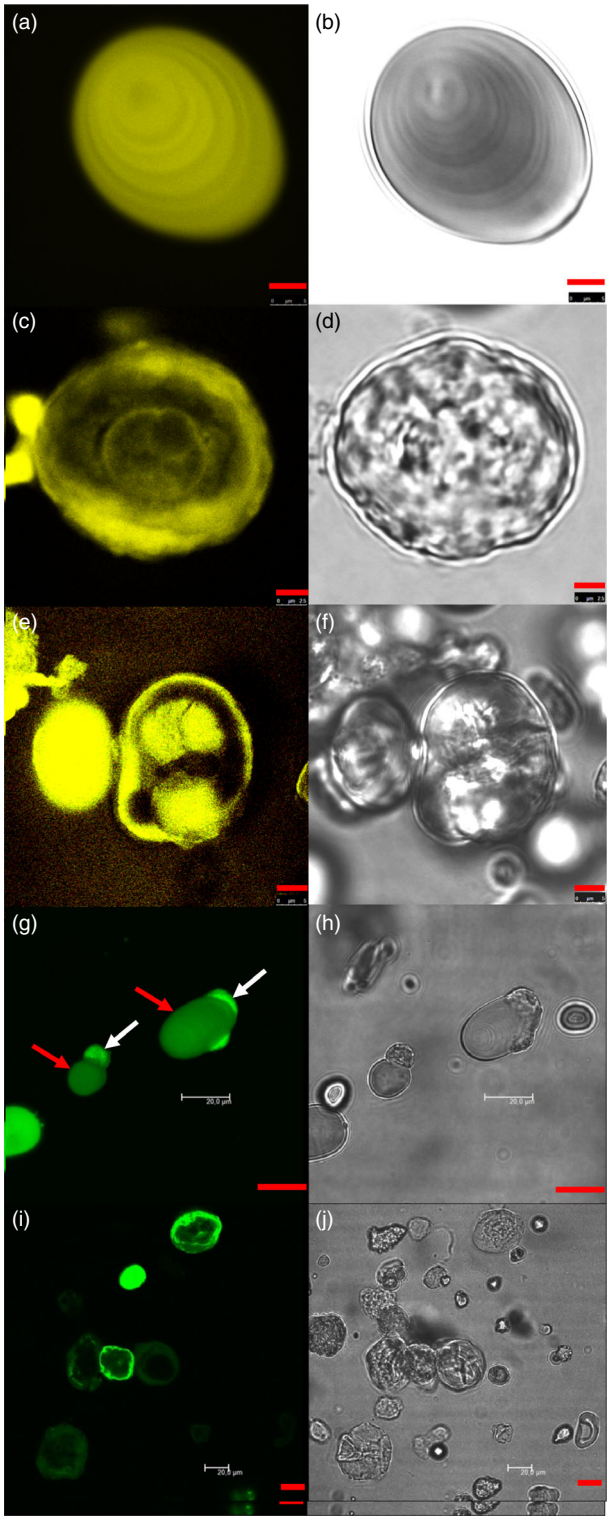

Figure 1 Confocal microscopic analysis of starch granules from selected lines. Cultivar Katinka granule stained with Safranin O (a) and bright field (b) (size bars 5 μm), IAm line 12-713-7 granule stained with Safranin O (c) and bright field (d) (size bars 25 μm), IAm line 12-713-7 granule stained with Safranin O (e) and bright field (f) (size bars 5 μm), IAm line 12-739-4 granules stained with APTS (g,i) and bright field (h,j) (scale bars 20 μm). Red arrows (g) indicate normal granule morphology and white arrows apposition of amylose-rich material.

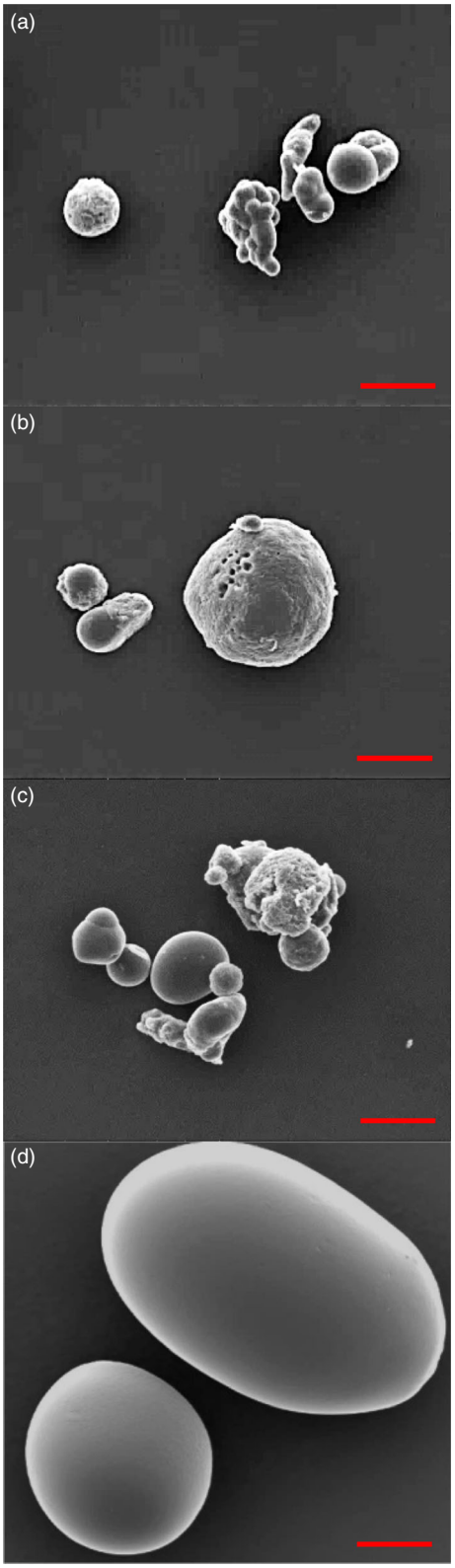

Figure 2 Scanning electron micrographs (SEM). (a) IAm line 12-723-1 representing high-amylose IAm lines with multiple granule intitiation, (b) IAm line 12-713-7 representing high-amylose IAm lines with highly disorganised granules, (c) IAm line 12-739-4 representing least amylose lines with partly normal starch granules and (d) control cultivar Katinka.

Table 4 Pasting parameters (RVA)

Line	PV	HPV	BD	FV	SB	PT
Stabilo	2690	1350	1340	1570	216	68.7
Katinka	2540	1200	1340	1380	175	68.7
93-CAL-3	3520	1680	1840	1890	209	69.4
94-BVB-6	2390	1590	802	1810	224	70.3
Oleva	nd	nd	nd	nd	nd	nd
12-702-2	501	462	39	956	494	80.1
12-702-3	260	242	18	457	215	78.8
12-702-8	413	390	23	704	314	79.1
12-712-6	nd	nd	nd	nd	nd	nd
12-712-8	242	230	12	389	159	78.7
12-713-3	151	141	10	255	114	69.9
12-713-7	nd	nd	nd	nd	nd	nd
12-715-5	142	123	19	264	141	71.7
12-716-1	140	125	15	233	108	70.3
12-723-1	149	140	9	252	112	75.5
12-727-6	101	94	7	160	66	77.5
12-739-4	420	389	31	716	327	95.3

PV, Peak viscosity; HPV, hot paste viscosity; BD, breakdown; FV, final viscosity; SB, setback, PT, pasting temperature; nd, not determined. Parameters are described in the Experimental Procedures section.

020699) being 556-fold down-regulated in the IAm lines as compared to the control lines (FDR corrected *P*-value 1.15×10^{-26}). This is in agreement with the presence of this starch metabolism gene on the homozygous region on chromosome 7. Indeed, among the 186 differentially expressed genes, 34 were found located on chromosome 7. This represents a significant enrichment of genes located in this region (χ^2 *P*-value: 0.001) consistent with this large region on chromosome 7 originating from *S. sandemanii* and not from the control group of *S. tuberosum* backcrossing lines. No other chromosomes showed a significant overrepresentation of differentially expressed genes including chromosomes 3 and 10. The second candidate gene from chromosome 7, ADP-glucose pyrophosphorylase large subunit AGPaseS-7 (PGSC0003DMG400015952), did not show any difference in expression. A third gene encoding isoamylase on chromosome 10, PGSC0003DMG400030253 (18-fold down-regulated in IAm lines (FDR corrected *P*-value 0.003), was also found differentially regulated. However, the gene on chromosome 10 appears truncated, and we speculate that this locus may be a pseudogene originating from the chromosome 7 locus or an error in the genome assembly. As annotated, it is not likely to give rise to a functional isoamylase and may not even be truly expressed and the expression values obtained in the RNA sequencing experiment may be an artefact caused by crossmapping of RNA-Seq reads among the two highly homologous loci. Taken together, the transcriptomic and genomic data strongly support isoamylase isoform 1 DBE-7 (PGSC0003DMG400 020699) as a candidate gene for the IAm phenotype and that loss of mRNA synthesis from this locus is the mechanism of loss of enzyme activity (see below).

Activity gel electrophoresis for debranching enzyme activity

All parental lines had three main regions of activity on the gel, an upper band, a middle band and a weak lower band region (Figure 5). All the IAm lines, except for sample 13 (line 12-712-8), were devoid of an upper band. According to Bustos *et al.* (2004), this activity band corresponds to the Stisa1/2 complex. The upper band in the Sample 13 line, however, was not located at the same position as the control bands suggesting that this band does not represent Stisa1/2 activity. Hence, all the lines having the *S. sandemanii* DNA are lacking the Stisa1/2 activity, which is in accordance with the lack of debranching enzyme isoamylase isoform 1 DBE-7 gene coding for the Stisa1 protein as deduced from the genomic and expression analysis. Intriguingly, RNAi suppression of Stisa1 does not generate the phenotype we found (Bustos *et al.*, 2004); hence, the almost complete suppression of Stisa1/2 activity in the IAm lines as deduced from the AGE analysis in combination with increased granule-bound Pho1 activity and suppressed SS activity (Krunic *et al.*, 2017) is therefore prospectively the cause for the IAm observed phenotype.

Discussion

The data in this study demonstrate the effects of introgression of a recessive allele from *S. sandemanii*, highly backcrossed in tetraploid *S. tuberosum* on starch biosynthesis and an increase in amylose (IAm) and tuber sugars. In a pool of BC4 tetraploid lines having increased amylose content, three large genomic regions on chromosomes 3, 7 and 10 showed reduced heterozygosity. The loss of heterozygosity in regions of the genome does not appear to stem from large scale deletions, because the read coverage in low heterozygosity regions is similar to high heterozygosity regions. This suggests that indeed the loss of heterozygosity is caused by increased causal allele dosis in these regions, which would also be the simplest expected genetics from a recessive trait. Within these regions, only two credible starch metabolism-related genes were found, that is one starch debranching enzyme 1 and one ADP-glucose pyrophosphorylase large subunit AGPase gene. Since the latter sequence did not show any difference in gene expression whereas the former showed a 500-fold decrease in gene expression, we hypothesize that the IAm phenotype mainly originates from the starch debranching enzyme 1 (Stisa1) deficiency.

This hypothesis was further supported by observed decreased Stisa1/2 complex activity measured by AGE analysis. The observed small and distorted starch granules in the IAm lines indicate a higher rate of initiation of granule biosynthesis supporting a direct effect of suppressed ISA activity in that process as suggested by Bustos *et al.* (2004). However, previously antisense suppression of Stisa1 or Stisa2 in potato tubers resulted in accumulation of phytoglycogen and did not result in major alterations of chain-length profiles of the starch nor in misshaped starch granules (Bustos *et al.*, 2004). We therefore speculate that the difference in starch granule appearance may be caused by a small amount of residual Stisa1 activity following antisense in contrast to the

Figure 3 Comprehensive microarray polymer profiling (CoMPP) heat map. The probes used (in parenthesis) are as described (Moller *et al.*, 2007; Pedersen *et al.*, 2012). HG: homogalacturonan; AGP: arabinogalactan proteins; and CBM20: carbohydrate-binding module family 20 recognizing starch. Values indicate relative intensity of signal, the highest value set to a 100. AIR: alcohol insoluble residue. Low viscosity samples: samples de-starched by treatment with Termamyl.

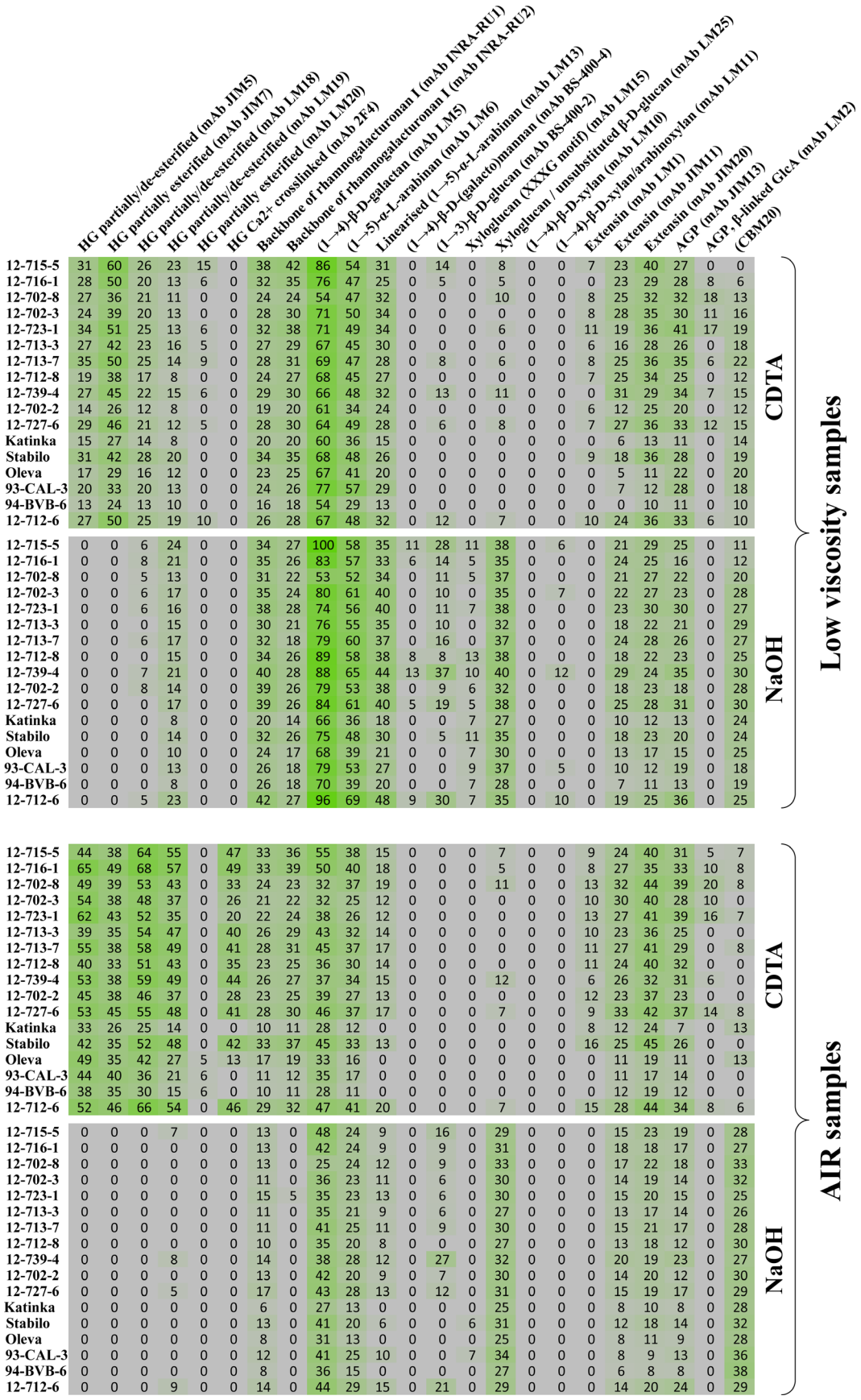
HG partially/de-esterified (mAb JIM5)
HG partially esterified (mAb JIM7)
HG partially/de-esterified (mAb LM18)
HG partially/de-esterified (mAb LM19)
HG partially esterified (mAb LM20)
HG Ca2+ crosslinked (mAb 2F4)
Backbone of rhamnogalacturonan I (mAb INRA-RU1)
Backbone of rhamnogalacturonan I (mAb INRA-RU2)
(1→4)-β-D-galactan (mAb LM5)
(1→5)-α-L-arabinan (mAb LM6)
Linearised (1→5)-α-L-arabinan (mAb LM13)
(1→4)-β-D-(galacto)mannan (mAb BS-400-4)
(1→3)-β-D-glucan (mAb BS-400-2)
Xyloglucan (XXXG motif) (mAb LM15)
Xyloglucan / unsubstituted β-D-glucan (mAb LM25)
(1→4)-β-D-xylan (mAb LM10)
(1→4)-β-D-xylan/arabinoxylan (mAb LM11)
Extensin (mAb LM1)
Extensin (mAb JIM11)
Extensin (mAb JIM20)
AGP (mAb JIM13)
AGP, β-linked GlcA (mAb LM2) (CBM20)
12-715-5 31 60 26 23 15 0 38 42 86 54 31 0 14 0 8 0 0 7 23 40 27 0 0
12-716-1 28 50 20 13 6 0 32 35 76 47 25 0 5 0 5 0 0 0 23 29 28 8 6
12-702-8 27 36 21 11 0 0 24 24 54 47 32 0 0 0 10 0 0 8 25 32 32 18 13
12-702-3 24 39 20 13 0 0 28 30 71 50 34 0 0 0 0 0 0 8 28 35 30 11 16
12-723-1 34 51 25 13 6 0 32 38 71 49 34 0 0 0 6 0 0 11 19 36 41 17 19
12-713-3 27 42 23 16 5 0 27 29 67 45 30 0 0 0 0 0 0 6 16 28 26 0 18
12-713-7 35 50 25 14 9 0 28 31 69 47 28 0 8 0 6 0 0 8 25 36 35 6 22
12-712-8 19 38 17 8 0 0 24 27 68 45 27 0 0 0 0 0 0 7 25 34 25 0 12
12-739-4 27 45 22 15 6 0 29 30 66 48 32 0 13 0 11 0 0 0 31 29 34 7 15
12-702-2 14 26 12 8 0 0 19 20 61 34 24 0 0 0 0 0 0 6 12 25 20 0 12
12-727-6 29 46 21 12 5 0 28 30 64 49 28 0 6 0 8 0 0 7 27 36 33 12 15
Katinka 15 27 14 8 0 0 20 20 60 36 15 0 0 0 0 0 0 0 6 13 11 0 14
Stabilo 31 42 28 20 0 0 34 35 68 48 26 0 0 0 0 0 0 9 18 36 28 0 19
Oleva 17 29 16 12 0 0 23 25 67 41 20 0 0 0 0 0 0 0 5 11 22 0 20
93-CAL-3 20 33 20 13 0 0 24 26 77 57 29 0 0 0 0 0 0 0 7 12 28 0 18
94-BVB-6 13 24 13 10 0 0 16 18 54 29 13 0 0 0 0 0 0 0 0 10 11 0 10
12-712-6 27 50 25 19 10 0 26 28 67 48 32 0 12 0 7 0 0 10 24 36 33 6 10
12-715-5 0 0 6 24 0 0 34 27 100 58 35 11 28 11 38 0 6 0 21 29 25 0 11
12-716-1 0 0 8 21 0 0 35 26 83 57 33 6 14 5 35 0 0 0 24 25 16 0 12
12-702-8 0 0 5 13 0 0 31 22 53 52 34 0 11 5 37 0 0 0 21 27 22 0 20
12-702-3 0 0 6 17 0 0 35 24 80 61 40 0 10 0 35 0 7 0 22 27 23 0 28
12-723-1 0 0 6 16 0 0 38 28 74 56 40 0 11 7 38 0 0 0 23 30 30 0 27
12-713-3 0 0 0 15 0 0 30 21 76 55 35 0 10 0 32 0 0 0 18 22 21 0 29
12-713-7 0 0 6 17 0 0 32 18 79 60 37 0 16 0 37 0 0 0 24 28 26 0 27
12-712-8 0 0 0 15 0 0 34 26 89 58 38 8 8 13 38 0 0 0 18 22 23 0 25
12-739-4 0 0 7 21 0 0 40 28 88 65 44 13 37 10 40 0 12 0 29 24 35 0 30
12-702-2 0 0 8 14 0 0 39 26 79 53 38 0 9 6 32 0 0 0 18 23 18 0 28
12-727-6 0 0 0 17 0 0 39 26 84 61 40 5 19 5 38 0 0 0 25 28 31 0 30
Katinka 0 0 0 8 0 0 20 14 66 36 18 0 0 7 27 0 0 0 10 12 13 0 24
Stabilo 0 0 0 14 0 0 32 26 75 48 30 0 5 11 35 0 0 0 18 23 20 0 24
Oleva 0 0 0 10 0 0 24 17 68 39 21 0 0 7 30 0 0 0 13 17 15 0 25
93-CAL-3 0 0 0 13 0 0 26 18 79 53 27 0 0 9 37 0 5 0 10 12 19 0 18
94-BVB-6 0 0 0 8 0 0 26 18 70 39 20 0 0 7 28 0 0 0 7 11 13 0 19
12-712-6 0 0 5 23 0 0 42 27 96 69 48 9 30 7 35 0 10 0 19 25 36 0 25
12-715-5 44 38 64 55 0 47 33 36 55 38 15 0 0 0 7 0 0 9 24 40 31 5 7
12-716-1 65 49 68 57 0 49 33 39 50 40 18 0 0 0 5 0 0 8 27 35 33 10 8
12-702-8 49 39 53 43 0 33 24 23 32 37 19 0 0 0 11 0 0 13 32 44 39 20 8
12-702-3 54 38 48 37 0 26 21 22 32 25 12 0 0 0 0 0 0 10 30 40 28 10 0
12-723-1 62 43 52 35 0 20 22 24 38 26 12 0 0 0 0 0 0 13 27 41 39 16 7
12-713-3 39 35 54 47 0 40 26 29 43 32 14 0 0 0 0 0 0 10 23 36 25 0 0
12-713-7 55 38 58 49 0 41 28 31 45 37 17 0 0 0 0 0 0 11 27 41 29 0 8
12-712-8 40 33 51 43 0 35 23 25 36 30 14 0 0 0 0 0 0 11 24 40 32 0 0
12-739-4 53 38 59 49 0 44 26 27 37 34 15 0 0 0 12 0 0 6 26 32 31 6 0
12-702-2 45 38 46 37 0 28 23 25 39 27 13 0 0 0 0 0 0 12 23 37 23 0 0
12-727-6 53 45 55 48 0 41 28 30 46 37 17 0 0 0 7 0 0 9 33 42 37 14 8
Katinka 33 26 25 14 0 0 10 11 28 12 0 0 0 0 0 0 0 8 12 24 7 0 13
Stabilo 42 35 52 48 0 42 33 37 45 33 13 0 0 0 0 0 0 16 25 45 26 0 0
Oleva 49 35 42 27 5 13 17 19 33 16 0 0 0 0 0 0 0 0 11 19 11 0 13
93-CAL-3 44 40 36 21 6 0 11 12 35 17 0 0 0 0 0 0 0 0 11 17 14 0 0
94-BVB-6 38 35 30 15 6 0 10 11 28 11 0 0 0 0 0 0 0 0 12 19 12 0 0
12-712-6 52 46 66 54 0 46 29 32 47 41 20 0 0 0 7 0 0 15 28 44 34 8 6
12-715-5 0 0 0 7 0 0 13 0 48 24 9 0 16 0 29 0 0 0 15 23 19 0 28
12-716-1 0 0 0 0 0 0 13 0 42 24 9 0 9 0 31 0 0 0 18 18 17 0 27
12-702-8 0 0 0 0 0 0 13 0 25 24 12 0 9 0 33 0 0 0 17 22 18 0 33
12-702-3 0 0 0 0 0 0 11 0 36 23 11 0 6 0 30 0 0 0 14 19 14 0 32
12-723-1 0 0 0 0 0 0 15 5 35 23 13 0 6 0 30 0 0 0 15 20 15 0 25
12-713-3 0 0 0 0 0 0 11 0 35 21 9 0 6 0 27 0 0 0 13 17 14 0 26
12-713-7 0 0 0 0 0 0 11 0 41 25 11 0 9 0 30 0 0 0 15 21 17 0 28
12-712-8 0 0 0 0 0 0 10 0 35 20 8 0 0 0 27 0 0 0 13 18 12 0 30
12-739-4 0 0 0 8 0 0 14 0 38 28 12 0 27 0 32 0 0 0 20 19 23 0 27
12-702-2 0 0 0 0 0 0 13 0 42 20 9 0 7 0 30 0 0 0 14 20 12 0 30
12-727-6 0 0 0 5 0 0 17 0 43 28 13 0 12 0 31 0 0 0 15 19 17 0 29
Katinka 0 0 0 0 0 0 6 0 27 13 0 0 0 0 25 0 0 0 8 10 8 0 28
Stabilo 0 0 0 0 0 0 13 0 41 20 6 0 0 6 31 0 0 0 12 18 14 0 32
Oleva 0 0 0 0 0 0 8 0 31 13 0 0 0 0 25 0 0 0 8 11 9 0 28
93-CAL-3 0 0 0 0 0 0 12 0 41 25 10 0 0 7 34 0 0 0 8 9 13 0 36
94-BVB-6 0 0 0 0 0 0 8 0 36 15 0 0 0 0 27 0 0 0 6 8 8 0 38
12-712-6 0 0 0 9 0 0 14 0 44 29 15 0 21 0 29 0 0 0 14 20 24 0 29
CDTA
NaOH
Low viscosity samples
CDTA
NaOH
AIR samples

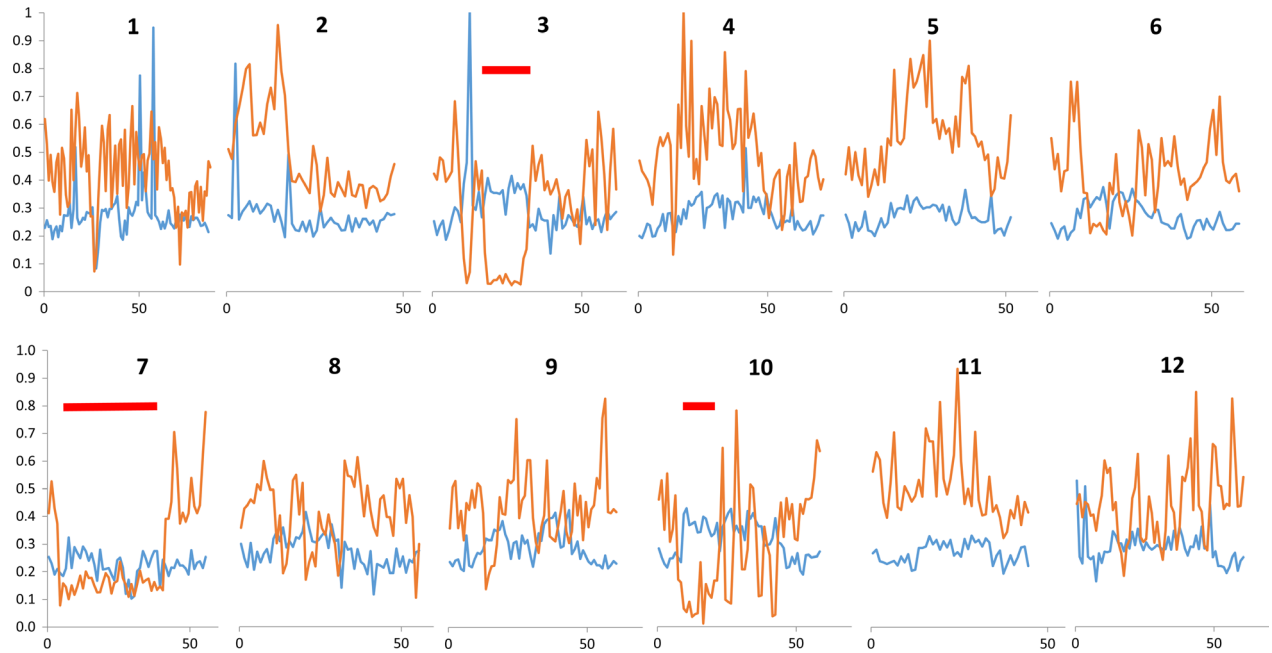

Figure 4 Genome-wide heterozygosity. Ratio of heterozygous SNPs/total SNPs in 1 Mbp bins is shown in orange. Average coverage in the same bins is shown in blue. *X*-axis is Mbp. Regions of low heterozygosity are marked by solid red lines (see main text for details).

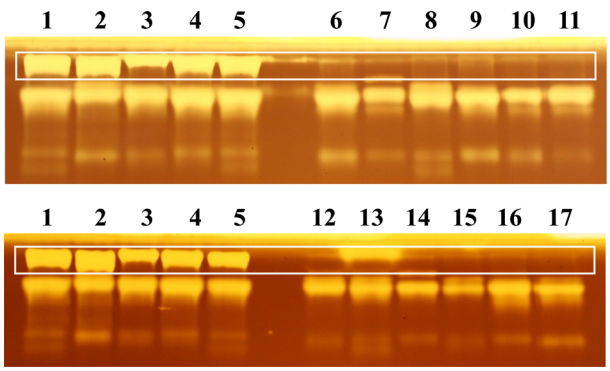

Figure 5 AGE of debranching enzyme activity demonstrating the absence of Stisa1/2 activity (boxed). 1-5: control lines. 1: 93-CAL-3; 2: 94-BVB-6; 3: Katinka; 4: Stabilo; 5: Oleva; 6: 12-715-5; 7: 12-716-1; 8: 12-702-8; 9: 12-702-3; 10: 12-723-1; 11: 12-713-3; 12: 12-713-7; 13: 12-712-8; 14: 12-739-4; 15: 12-702-2; 16: 12-727-6; and 17: 12-712-6. Control lines shown in duplicate, one for each gel.

abolishment of Stisa1 expression by our homozygous IAm lines. However, considering the complexity of starch metabolism in potato, we cannot rule out that the IAm lines are also affected by additional enzyme activities. Notably, we previously demonstrated that phosphorylase1 (Pho1) shifted in molecular size and its granule-bound activity increased and soluble starch synthase (SS), but not the granule-bound starch synthase (GBSS), decreased (Krunic *et al.*, 2017). SS suppression can result in structural alteration in the amylopectin, and for example, changes in amylopectin chain-length distribution in high-amylose lines of rice double mutants lacking SSI and SSIIIa (Fujita *et al.*, 2011) and SSII/SSIII antisense potato suppressor lines (Edwards *et al.*, 1999; Lloyd *et al.*, 1999) are similar to the structural effects of the IAm lines. Like ISA, Pho1 is suggested to be involved in starch granule initiation (Subashinghe et al., 2014) the increased Pho1 activity found in the IAm lines (Krunic *et al.*, 2017) can explain the higher number of small starch granules. However, a possible link between Pho1-driven starch biosynthesis and the increased amylose chemotype is not clear. Pho1 has high catalytic activity towards linear glucans (Steup and Schachtele, 1981), and high starch-bound Pho1 activity could therefore be associated with high amylose since Pho1is found to be more granule-bound in high-amylose barley genotypes (Subashinghe *et al.*, 2014). In support for specific roles of SS and Pho1, two alternative pathways of starch biosynthesis can be suggested, driven by SSs and Pho1, respectively, active at different temperature regimes (Fettke *et al.*, 2010; Fettke *et al*, 2012; Kaminski *et al.*, 2012). Our data are in agreement with a re-directed starch biosynthesis towards an alternative Pho1-driven route at the expense of the SS route, and the absence of Stisa1/2 in the IAm lines likely provides additional effects on amylopectin structure and starch and amylose contents. In Arabidopsis, loss of isoamylase activity leads to phytoglycogen formation, but additional loss of a specific alpha-amylase (AMY8) effectively restores starch formation (Streb *et al.*, 2008). Tuber amylolytic activity, as indicated by activity gel electrophoresis (Krunic *et al.*, 2017), was inconsistently varied in tubers among the IAm lines. Hence, specific amylase activity including a potential Arabidopsis Amy8 homologue, reverting biosynthesis of granular starch in the Stisa-deficient tubers, is not likely. The higher starch phosphate levels found were persistent over the BC generations and can be directly linked to a decrease in the inactive, granule-bound GWD1 protein in the IAm lines (Krunic *et al.*, 2017).

Tuber morphology was substantially changed in many of the lines. Such changes can be due to effects on cell wall metabolism and structure as demonstrated by CoMPP analysis. Specifically, increased expression of specific AGPs as we found in IAm lines can indicate increased plasticity and expansion potential of the cell walls among other effects identified elsewhere (as summarized in Ellis *et al.*, 2010).

Enzymes of starch biosynthesis are present as dynamic protein complexes. Pho1 in maize forms a complex with SBE (Hennen-Bierwagen *et al.*, 2009) and also seems to interact with other starch biosynthetic enzymes and connects enzymes in these complexes (Liu *et al.*, 2009; Tetlow *et al.*, 2004; Zhang *et al.*, 2011). Interestingly, changes in such enzyme complexes are often linked to high-amylose phenotypes (Subashige *et al.,* 2014) and prevention of complex formation can result structural differences of the product including increased amylose and altered amylopectin chain-length distributions as we observed in this study. The complete suppression of Stisa1/2 activity identified in this study, possibly combined with increased granule-bound pho activity and reduced SS activity, is likely together responsible for the specific IAm phenotype.

Experimental procedures

Plant growth and tuber harvest

Potato tubers were produced in a regular field (Ikast, Denmark) from the end of April 2014 and were harvested mid-September 2014. This material was used for starch extraction and starch chemical, physical and degradation analyses. Tubers were also produced and freshly harvested in greenhouse, where plants were grown in soil in pots under ambient conditions and with supplementing light for analysis of enzyme activity, DNA sequencing and transcriptome analysis. For these experiments, potato tubers were harvested from 3-month-old plants, washed and sliced in 1 cm dices, frozen in liquid nitrogen and stored at −80 °C freezer until analysis.

Plant selection and crossing

Tetraploid *S. tuberosum* lines (15 lines) homozygous for a DNA string derived from the diploid wild species *S. sandemanii* (Schittenhelm and Menge-Hartmann, 1992), accession number GCN17600, lacking a 454 bp AFLP sequence were generated as described (Krunic *et al.*, 2017). Further backcrosses to different tetraploid *S. tuberosum* cultivars alternated with intercrossing were carried out according to schedule in Table S1 for production of 15 new IAm lines with less *S. sandemanii* genes but still containing the string lacking the 454 bp sequence. The crossings are referred to backcrossing (BC) 1 to 4 (BC1, BC2, BC3 and BC4) following the original F1 crossing, BC3, having a calculated 6.25% of *S. sandemanii* DNA and BC4 having a calculated 3.125% of *S. sandemanii* DNA.

Starch extraction

Starch was isolated from freshly harvested tubers using a fruit juicer (Moulinex 753). Na_2SO_3 (0.04 M) was added to prevent oxidation and the starch was left to sediment. The juice was decanted and the starch was washed twice with 10 volumes sodium phosphate buffer (0.05 M, pH 6.5) and twice with 10 volumes of Milli-Q water. Between washes the starch was left to sediment at 5 °C overnight. After the final wash, the starch was sieved through a 140 μm steel mesh followed by a 100 μm steel mesh. After sedimentation and decanting, the starch was dried for 3 days at room temperature.

Starch content

Frozen potato tubers were powdered in a mortar in liquid nitrogen; 5 mg powdered samples were used for analysis. Soluble sugars were removed by extraction five times in 80% (v/v) ethanol at 80 °C, with intermittent centrifugation at 10 000 ***g*** for 5 min. The powder was suspended in 200 μL of 2 M KOH with constant mixing by magnetic stirrer on ice for 20 min. The suspension was adjusted to pH 3.8 by adding 800 μL of 1.2 M sodium acetate buffer (pH 3.8) and incubated for 5 min at 80 °C. Heat-stable α-amylase (0.1 KNU-T units of Termamyl, Novozymes, Denmark) was added and the samples were incubated for 3 h at 80 °C. The samples were cooled to 60 °C, and 0.3 AGU units of amyloglucosidase (Dextrozyme, Novozymes, Denmark) were added to samples. Samples were incubated at 60 °C overnight, with constant mixing. After centrifugation (20 000 ***g*** for 5 min), the supernatant was analysed for glucose using PGO enzymes (Sigma-Aldrich) using glucose as a standard. The analysis was performed in biological triplicates.

Free sugars

Sugars were extracted from tubers by heating 200 mg tuber material with 1 mL 80% ethanol to 80 °C for 2 h. The supernatant was collected, and another 0.5 mL ethanol was added to the tuber and heated to 80 °C for 2 h. The two supernatants were pooled and centrifuged (13 000 ***g***, 5 min). The liquid was collected and dried under vacuum (30 °C). The pellet was resuspended in 200 μL H_2O and analysed by high-performance anion-exchange chromatography as described (Lunde *et al.*, 2008). The analysis was done in triplicates.

Apparent amylose

Apparent amylose content, not discriminating the presence of possible long chains in the amylopectin fraction, was determined by iodine colorimetry using standard starches as described earlier (Wickramasinghe *et al.*, 2009).

Amylopectin chain-length distribution

Samples were gelatinized by boiling and enzymatically debranched by using 0.24U of isoamylase per 5 mg of sample at 40 °C. A 20 μL sample aliquot of such linearized α-glucan (100 μg of linear α-glucan) was analysed by high-pressure anion-exchange chromatography with pulsed amperometric detection (HPAEC-PAD, Dionex, Sunnyvale, CA) as described (Blennow *et al.*, 1998).

Starch phosphate content

The content of C-3 and C-6 mono-esterified phosphate groups to the starch was analysed using HPAEC-PAD as described earlier (Carciofi *et al.*, 2011), and concentrations given as nmole Glc6-P and Glc3-P/mg starch.

Starch granule size distribution

The starch granule size distribution was determined by laser diffraction of starch slurries in water and analysed using a Microtrac S3000 analyzer (Microtrac, PA). Approximately 50 mg of sample was analysed and the samples were exposed to sonication in a sonication bath for 10 min prior to analysis to avoid aggregation. The data were analysed using Microtrac Flex Software and extracted as granule size distribution based on volume distribution mean diameter (MV), number distribution (MN) and area distribution (MA) (the two latter calculated based on the fraction of granule size classes of the overall distribution, in this case based on the fractions of the total number or granule area of the granules, respectively) and graphic standard deviation (SD).

Microscopy

Starch granule morphology and topography were studied by scanning electron microscopy (SEM) which was conducted as

described previously (Carciofi *et al.*, 2011). Inner structural features of starch granules were studied by confocal laser scanning microscopy (CLSM) mainly as described (Blennow *et al.*, 2003) using 8-amino-1,3,6-pyrenetrisulfonic acid (APTS) for reducing end labelling visualizing mainly amylose. To provide a general staining of the granules revealing the cavital structure, granules were soaked in Safranin O for 5 min at ambient temperature followed by washing 3 times with excess Milli-Q water. For SEM, starch granules were mounted on carbon tabs on aluminium stubs. Samples were sputter coated with gold/palladium for 120 s and observed with secondary detector at an accelerating voltage 10 kV in Quanta 200 SEM (FEI Company, Eindhoven, Netherlands).

RVA analysis

Pasting profiles of the starch samples were analysed using Rapid Visco Analyser (RVA, model 4; Newport Scientific, Warriewood, Australia) as described (Blennow *et al.*, 2005). Parameters calculated for the pasting curves were peak viscosity (PV), hot paste viscosity (HPV), breakdown (BD), final viscosity (FV), setback (SB) and pasting temperature (PT). PV is the highest peak of the viscogram, HPV the trough viscosity following the PV, FV the end-point viscosity, SB the difference between the FV and HPV indicating molecular reassociation and PT the temperature of gelatinization of the starch.

In vitro enzymatic starch hydrolysis

In vitro starch degradation kinetics was analysed by a modification of the Englyst method (Englyst *et al.*, 1992), using gelatinized starch granules (98 °C, 12 min). Starch samples (2% in 250 μL) were incubated in triplicates with 2U of each α-amylase from porcine pancreas (Sigma A3176) and amyloglucosidase (*A. niger*, Fluka 10113) in 20 mM sodium phosphate buffer (pH 6.0) with 6.7 mM sodium chloride at 37 °C for 0, 0.5, 1, 2, 3 and 4 h. The treatment without incubation is taken as a control. Enzyme treatment was terminated by adding 30 μL 0.1 M HCl and 250 μL of 50% ethanol on ice, centrifuged (14 000 ***g***, 5 min) and the supernatant was collected. The amount of glucose released from starch hydrolysis was measured using the PGO enzymes kit (Sigma-Aldrich), glucose as standard and the conversion factor of 0.9 to calculate the mass of starch from glucose data. The rate of starch hydrolysis was expressed as the per cent of total starch at the end of each interval. RS was calculated as total starch (100% being the % of starch hydrolysed within 120 min).

Comprehensive microarray polymer profiling (CoMPP): Microarray printing, microarray probing and analysis

Sample preparation from tissue

Tuber tissue was snap-frozen in liquid nitrogen, freeze-dried and powdered using a mortar and a pestle in liquid nitrogen. This sample is referred to as low viscosity. Part of this material was sequentially extracted with 70% ethanol, 1:1 methanol:chloroform and acetone in the ratio 50 mg to 1.5 mL of solvent to obtain alcohol insoluble residue (AIR). De-starched, low viscosity sample was prepared by dissolving 20 mg of AIR in 400 μL of 50 mM MOPS pH 7.0 with 3 units/mL of Termamyl. Samples were incubated for 10 min at 85 °C and quickly cooled down to room temperature and precipitated with 1 mL of 96% ethanol. The sample was spun at 15 000 ***g*** at 4 °C for 10 min and the supernatant was discarded. The pellet was washed with acetone and left to air-dry.

CoMPP analysis

Glycans from 10 mg tissue were sequentially extracted with 50 mM diamino-cyclo-hexane-tetra-acetic acid (CDTA) and 4 M NaOH (Moller *et al.*, 2007; Pedersen *et al.*, 2012), and microarrays were printed on nitrocellulose membrane (Whatman 0.45 μm) diluted in buffer containing 55.2% glycerol, 44.0% water, 0.8% Triton X-100 and printed with four fivefold dilutions and with two technical replicates to a total of 8 spots as described (Moller *et al.*, 2007; Pedersen *et al.*, 2012) using a piezoelectric Arrayjet Sprint (Arrayjet, Roslin, UK). The arrays were blocked in PBS (phosphate-buffered saline) containing 5% v/w milk powder. Following, the arrays were probed with primary antibody and detected with anti-mouse and anti-rat secondary antibodies conjugated to alkaline phosphatase (Sigma, Poole, UK) diluted 1/5000 in 5% MPBS. Probed arrays were developed using 5-bromo-4-chloro-3-indolylphosphate and nitro blue tetrazolium in alkaline phosphatase buffer. Microarrays were quantified using Array-Pro Analyser (Media Cybernetics) and presented as heat maps in which colour intensity was correlated to mean spot signals. For each heat map, the highest value was set to a 100 and the rest adjusted accordingly and a cut-off of 5 was introduced.

Genomic DNA analysis

Leaf samples from 15 selected greenhouse-grown potato lines (Table S1) were harvested, immediately frozen in liquid nitrogen and stored at −80 °C until further processing. DNA extraction was performed separately for each line by homogenizing 100–200 mg of leaf tissue by subjecting the sample to three cycles of 10 s (with 5 s breaks) homogenization at 6500 rpm using a Precellys mechanical homogenizer (Bertin Technologies, France) in a Precellys CK14 tissue homogenization tube with metal beads. Genomic DNA was purified using the DNeasy plant mini kit according to the manufacturer's instructions. DNA purity was evaluated by 1% TAE-agarose gel electrophoresis) and spectroscopic analysis by NanoDrop® Spectrophotometer ND-1000 (Thermo Scientific, Wilmington, DE). Subsequently, PicoGreen® dsDNA quantitation permitted pooling of equal amounts of DNA from each sample prior to DNA sequencing using the TruSeq preparation kit and paired-end sequencing 2 × 150 bp on a HiSeq 2000 sequencer (Illumina, San Diego, CA).

The resulting sequence reads were mapped using the Genomics Workbench v 6.5.1 (CLC Bio, Aarhus, Denmark), quality trimming (limit = 0.05, maximum, number of ambiguous nucleotides = 2) and read mapping (minimum length fraction = 0.8, minimum similarity fraction = 0.8, random matching allowed, otherwise default settings) of both pools individually against the potato reference genome pseudomolecule model (DM version 4.03 available at http://solanaceae.plantbiology.msu.edu/pgsc_download.shtml; Sharma *et al.*, 2013; Potato Genome Sequencing Consortium, 2011). Heterozygosity was estimated by calling biallelic SNPs using CLC Genomics Workbench v 6.5.1 (probabilistic variant caller; max read overage 250; min read coverage 100; min coverage of genotype 10; min % for each genotype, 12.5% for total SNP and 37.5% for heterozygous SNP, respectively). The ratio of heterozygous SNPs per total SNPs (both homozygous and heterozygous, but different from the reference) were calculated genome wide in a 5 Mbp sliding window for all 12 chromosomes.

Gene expression analysis

RNA was extracted from 15 IAm potato lines (Table S1) and the backcrossing lines/cultivars 93-Cal-3, Stabilo-T, Oleva and Katinka using the RNeasy kit (Qiagen, Hilden, Germany). Quality and quantity of RNA was assessed using a NanoDrop 1000 Spectrophotometer (Thermo Fisher Scientific, Waltham, MA) and TapeStation 2200 (Agilent Technologies, Santa Clara, CA) with the High Sensitivity RNA ScreenTape. The samples were processed using the TruSeq RNAv2 library prep kit and sequenced on a HiSeq2000 for 2x150 bp paired end. Following basecalling and demultiplexing, raw reads were imported into CLC workbench v 6.5.1 and mapped to potato reference genome (DM version 4.03 available at http://solanaceae.plantbiology.msu.edu/pgsc_download.shtml) (Potato Genome Sequencing Consortium, 2011; Sharma *et al.*, 2013) using the Large Gap Read Mapper module (Mismatch cost = 2, Insertion cost = 3, Deletion cost = 3, Length fraction = 0.8, Similarity fraction = 0.8, Global alignment = No, Auto-detect paired distances = Yes, Strand specific = Both, Maximum number of hits for a read = 10, Count paired reads as two = No, Expression value = RPKM, Calculate RPKM for genes without transcripts = No). Nonspecific matches were ignored. The data were normalized using the Quantile option and differentially expressed genes between the 15 IAm lines and the 4 control lines were identified using the empirical analysis of DGE option essentially as (McCarthy *et al.*, 2012) using FDR correction 0.05, excluding counts below 5.

Extract preparation and activity gel electrophoresis (AGE) electrophoresis

Proteins were extracted from frozen tuber material (see section Plant growth and tuber harvest) in ice-cold buffer (1 mL buffer for 500 mg tuber) containing 100 mM 2-(N morpholino) ethanesulphonic acid (MES) buffer pH 6.0, 1 mM EDTA, 50 mL L^{-1} ethylene glycol and 20 mM DTT supplemented with protease inhibitor tablets (1 per 50 mL, Roche, 05056489001) using a tissue lyser (Qiagen, frequency 30/s for 25 s). Insoluble material was pelleted by centrifugation at 14 000 ***g*** for 10 min at 4 °C and the supernatant was used immediately for AGE experiments. Electrophoresis gels were prepared as previously described (Zeeman *et al.*, 1998) using 0.3% (w/v) beta-limit dextrin (Megazyme) in the separating gel and a extract corresponding to 9 mg fresh weight was electrophorized at 120 V for 2 h at 4 °C with running buffer including 1 mM sodium thioglycolate (Sigma T0632). Gels were then washed twice in incubation buffer (100 mM MES pH 6.0, 1 mM $CaCl_2$, 1 mM $MgCl_2$, 50 mL/L ethylene glycol and 20 mM DTT) for 15 min and subsequently incubated in the same buffer supplemented with 20 mM DTT for 20 h at 30 °C. Activities were revealed after staining with iodide (0.34% I_2, 0.68% KI (w/v)).

Acknowledgements

This project was supported by Kartoffelafgiftsfonden, Denmark. We acknowledge Center for Advanced Bioimaging, Faculty of Science, University of Copenhagen for use of their microscopy facilities.

Conflict of interest

The authors declare no conflict of interest.

Authors' contribution

AB contributed to project coordination and manuscript writing. KS contributed to enzyme activity analysis. VT and SSS contributed to starch analysis. HGK involved in potato breeding. KLN and MSA were involved in genomics and transcriptomics. All authors contributed to manuscript writing.

References

Bird, A.R., Brown, I.L. and Topping, D.L. (2000) Starches, resistant starches, the gut microflora and human health. *Curr. Issu. Intest. Microbiol.* **1**, 25–37.

Blennow, A., Bay-Smidt, A.M., Wischmann, B., Olsen, C.E. and Møller, B.L. (1998) The degree of starch phosphorylation is related to the chain length distribution of the neutral and the phosphorylated chains of amylopectin. *Carbohydr. Res.* **307**, 45–54.

Blennow, A., Hansen, M., Schulz, A., Jørgensen, K., Donald, A.M. and Sanderson, J. (2003) The molecular deposition of transgenically modified starch as imaged by high-resolution microscopy. *J. Struct. Biol.* **143**, 229–241.

Blennow, A., Wischmann, B., Houborg, K., Ahmt, T., Madsen, F., Poulsen, P., Jørgensen, K. *et al.* (2005) Structure - function relationships of transgenic starches with engineered phosphate substitution and starch branching. *Int. J. Biol. Macromol.* **36**, 159–168.

Blennow, A., Jensen, S.L., Shaik, S.S., Skryhan, K., Holm, P.B., Hebelstrup, K.H. and Tanackovic, V. (2013) Future cereal starch bioengineering — Cereal ancestors encounter gene-tech and designer enzymes. *Cereal Chem.* **90**, 274–287.

Bustos, R., Fahy, B., Hylton, C.M., Seale, R., Nebane, N.M., Edwards, A., Martin, C. *et al.* (2004) Starch granule initiation is controlled by a heteromultimeric isoamylase in potato tubers. *Natl. Acad. Sci. Proc. USA*, **101**, 2215–2220.

Carciofi, M., Shaik, S.S., Jensen, S.L., Blennow, A., Svensson, J.T., Vincze, E. and Hebelstrup, K.H. (2011) Hyperphosphorylation of cereal starch. *J. Cereal Sci* **54**, 339–346.

Clasen, B., Voytas, D.F. and Zhang, F. (2015) *Potatoes with reduced granule-bound starch synthase*. Patent WO 2015193858 A1.

Damager, I., Engelsen, S.B., Blennow, A., Møller, B.L. and Motawia, S.M. (2010) First principles insight into starch-like α-glucans: their synthesis, conformation and hydration. *Chem. Rev.* **110**, 2049–2080.

Edwards, A., Fulton, D.C., Hylton, C.M., Jobling, S.A., Gidley, M., Rössner, U., and Martin, C. (1999) Combined reduction in activity of starch synthases II and III of potato has novel effects on the starch of tubers. *Plant J.* **17**, 251–261.

Ek, K.L., Wang, S.J., Copeland, L. and Brand-Miller, J.C. (2014) Discovery of a low-glycaemic index potato and relationship with starch digestion *in vitro*. *British J. Nutr.* **111**, 699–705.

Ellis, M., Egelund, J., Schultz, C.J. and Bacic, A. (2010) Arabinogalactan-proteins: key regulators at the cell surface? *Plant Physiol.* **153**, 403–419.

Englyst, H.N., Kingman, S.M. and Cummings, J.H. (1992) Classification and measurement of nutritionally important starch fractions. *Eur. J. Clin. Nutr.* **46**, 33–50.

Facon, M., Lin, Q., Azzaz, A.M., Hennen-Bierwagen, T.A., Myers, A.M., Putaux, J.L., Roussel, X. *et al.* (2013) Distinct functional properties of isoamylase-type starch debranching enzymes in monocot and dicot leaves. *Plant Physiol.* **163**, 1363–1375.

Fernandes, G., Velangi, A. and Wolever, T.M.S. (2005) Glycaemic index of potatoes commonly consumed in North America. *J. Am. Diet Assoc.* **105**, 557–562.

Fettke, J., Albrecht, T., Hejazi, M., Mahlow, S., Nakamura, Y. and Steup, M. (2010) Glucose 1-phosphate is efficiently taken up by potato (*Solanum tuberosum*) tuber parenchyma cells and converted to reserve starch granules. *New Phytol.* **185**, 663–675.

Fettke, J., Leifels, L., Brust, H., Herbst, K. and Steup, M. (2012) Two carbon fluxes to reserve starch in potato (*Solanum tuberosum* L.) tuber cells are closely interconnected but differently modulated by temperature. *J. Exp. Bot.* **63**, 3011–3029.

Fujita, N., Satoh, R., Hayashi, A., Kodama, M., Itoh, R., Aihara, S., and Nakamura, Y. (2011) Starch biosynthesis in rice endosperm requires the presence of either starch synthase I or IIIa. *J. Exp. Bot.* **62**, 4819–4831.

Giract organization (2011) *Starch Italics, 11th Ed*. http://issuu.com/giract/docs/starchitalics11.

Global Industry Analysts https://www.strategyr.com/market-report-starch-forecasts-global-industry-analysts-inc.asp

Hazard, B., Zhang, X.Q., Colasuonno, P., Uauy, C., Beckles, D.M., and Dubcovsky, J. (2012) Induced mutations in the starch branching enzyme ii (sbeii) genes increase amylose and resistant starch content in durum wheat. *Crop Sci.* **52**, 1754–1766.

Hennen-Bierwagen, T.A., Lin, Q., Grimaud, F., Planchot, V., Keeling, P.L., James, M.G., and Myers, A.M. (2009) Proteins from multiple metabolic pathways associate with starch biosynthetic enzymes in high molecular weight complexes: A model for regulation of carbon allocation in maize amyloplasts. *Plant Physiol.* **149**, 1541–1559.

Hennen-Bierwagen, T.A., James, M.G. and Myers, A.M. (2012) Involvement of debranching enzymes in starch biosynthesis. In *Starch, Origins, Structure and Metabolism, SEB Essential Review Series*, vol. **5** (Tetlow, I.J. ed), pp. 141–178. London, UK: Society for Experimental Biology.

Hofvander, P., Andersson, M., Larsson, C.T. and Larsson, H. (2004) Field performance and starch characteristics of high-amylose potatoes obtained by antisense gene targeting of two branching enzymes. *Plant Biotechnol. J.* **2**, 311–320.

Htoon, A., Shrestha, A.K., Flanagan, B.M., Lopez-Rubio, A., Birda, A.R., Gilbert, E.P. and Gidley, M.J. (2009) Effects of processing high amylose maize starches under controlled conditions on structural organisation and amylase digestibility. *Carbohydr. Polym.* **75**, 236–245.

Hussain, H., Mant, A., Seale, R., Zeeman, S., Hinchliffe, E., Edwards, A., Hylton, C. *et al*. (2002) Three isoforms of isoamylase contribute different catalytic properties for the debranching of potato glucans. *Plant Cell*, **15**, 133–149.

Johansen, I.E., Liu, Y., Jørgensen, B., Bennet, E.P., Nielsen, K.L., Blennow, A. and Petersen, B.L. (2019) High efficacy full allelic CRISPR/Cas9 gene editing in tetraploid potato. *Scientific Rep.* **9**, https://doi.org/10.1038/s41598-019-54126-w

Kaminski, K. P., Petersen, A. H., Sønderkær, M., Pedersen, L. H., Pedersen, H., Feder, C. and Nielsen, K. L. (2012) Transcriptome analysis suggests that starch synthesis may proceed via multiple metabolic routes in high yielding potato cultivars. *PloS One*, **7**, e51248.

Krunic, L., Skryhan, K., Mikkelsen, L., Ruzanski, C., Shaik, S.S., Kirk, H.-G., Palcic, M. *et al*. (2017) Non-GMO potato lines with re-directed starch biosynthesis pathway confers increased-amylose and resistant starch properties. *Starch-Starke*, **70**, 1600310.

Kubo, A., Colleoni, C., Dinges, J.R., Lin, Q.H., Lappe, R.R., Rivenbark, J.G., Meyer, A.J. *et al*. (2010) Functions of heteromeric and homomeric isoamylase-type starch-debranching enzymes in developing maize endosperm. *Plant Physiol.* **153**, 956–969.

Lee, B.H., Bello-Pérez, L.A., Lin, A.H.M., Kim, C.Y. and Hamaker, B.R. (2013) Importance of location of digestion and colonic fermentation of starch related to its quality. *Cereal Chem.* **90**, 335–343.

Liu, F., Makhmoudova, A., Lee, E.A., Wait, R., Emes, M.J., and Tetlow, I.J.. (2009) The amylose extender mutant of maize conditions novel protein-protein interactions between starch biosynthetic enzymes in amyloplasts. *J. Exp. Bot.* **60**, 4423–4440.

Lloyd, J.R., Landschütze, V. and Kossmann, J. (1999) Simultaneous antisense inhibition of two starch-synthase isoforms in potato tubers leads to accumulation of grossly modified amylopectin. *Biochem. J.* **338**, 515–521.

Lunde, C., Zygadlo, A., Simonsen, H.T., Nielsen, P.L., Blennow, A.,and Haldrup, A.. (2008) Sulfur starvation in rice: the effect on photosynthesis, sugar metabolism, and oxidative stress protective pathways. *Physiol. Plant.* **134**, 508–21.

McCarthy, D. J., Chen, Y. and Smyth, G.K. (2012) Differential expression analysis of multifactor RNA-Seq experiments with respect to biological variation. *Nucl. Acid Res.* **40**, 4288–4297.

Moller, I., Sørensen, I., Bernal, A.J., Blaukopf, C., Lee, K., Øbro, J. and Pettolino, F. (2007) High-throughput mapping of cell-wall polymers within and between plants using novel microarrays. *Plant J.* **50**, 1118–1128.

Nakamura, Y., Ono, M., Utsumi, C. and Steup, M. (2012) Functional interaction between plastidial starch phosphorylase and starch branching enzymes from rice during the synthesis of branched maltodextrins. *Plant Cell Physiol.* **53**, 869–878.

Pedersen, H.L., Fangel, J.U., McCleary, B., Ruzanski, C., Rydahl, M.G., Ralet, M.C., Farkas, V. *et al*. (2012) Versatile high resolution oligosaccharide microarrays for plant glycobiology and cell wall research. *J. Biol. Chem.* **287**, 39429–39438.

Perez, S. and Bertoft, E. (2010) The molecular structures of starch components and their contribution to the architecture of starch granules: A comprehensive review. *Starch/Staerke*, **62**, 389–420.

Regina, A., Bird, A., Topping, D., Bowden, S., Freeman, J., Barsby, T., Kosar-Hashemi, B. *et al*. (2006) High-amylose wheat generated by RNA interference improves indices of large bowel health in rats. *Natl. Acad. Sci. Proc. USA*, **103**, 3546–3551.

Regina, A., Blazek, J., Gilbert, E., Flanagan, B.M., Gidley, M.J., Cavanagh, C., Ral, J.P. *et al*. (2012) Differential effects of genetically distinct mechanisms of elevating amylose on barley starch characteristics. *Carbohydr. Polym.* **89**, 979–991.

Schittenhelm, S. and Menge-Hartmann, U. (1992) Stärke- und amylosegehalt sowie Größe und morphologie der Stärkekörner von knollentragenden *Solanum*-arten. *Landbauforsch. Völkenrode*, **42**, 117–126.

Schouten, H. and Jacobsen, E. (2008) Cisgenesis and intragenesis, sisters in innovative plant breeding. *Trends Plant Sci.* **13**, 260–261.

Schreiber, L., Nader-Nieto, A.C., Schönhals, E.M., Walkemeier, B. and Gebhardt, C. (2014) SNPs in genes functional in starch–sugar interconversion associate with natural variation of tuber starch and sugar content of potato (*Solanum tuberosum* L.) *G3 Genes Genomes. Genet.* **4**, 1797–1811.

Schwall, G.P., Safford, R., Westcott, R.J., Jeffcoat, R., Tayal, A., Shi, Y.C., Gidley, M.J. *et al*. (2000) Production of very-high-amylose potato starch by inhibition of SBE A and B. *Nat. Biotechnol.* **18**, 551–554.

Sestili, F., Janni, M., Doherty, A., Botticella, E., D'Ovidio, R., Masci, S., Jones, H.D. *et al*. (2010) Increasing the amylose content of durum wheat through silencing of the SBEIIa genes. *BMC Plant Biol.* **10**, 144.

Sharma, S.K., Bolser, D., de Boer, J., Sønderkær, M., Amoros, W., Carboni, M.F., D'Ambrosio, J.M. *et al*. (2013) Construction of reference chromosome-scale pseudomolecules for potato: integrating the potato genome with genetic and physical maps. *G3 Genes Genomes. Genet*. **3**, 2031–2047.

Shrestha, A.K., Ng, C.S., Lopez-Rubio, A., Blazek, J., Elliot, P., Gilbert, E.P., and Gidley, M.J. (2010) Enzyme resistance and structural organization in extruded high amylose maize starch. *Carbohydr. Polym.* **80**, 699–710.

Slade, A.J., McGuire, C., Loeffler, D., Mullenberg, J., Skinner, W., Fazio, G., Holm, A. *et al*. (2012) Development of high amylose wheat through TILLING. *BMC Plant Biol*. **12**, 1–17.

Steup, M. and Schachtele, C. (1981) Mode of glucan degradation by purified phosphorylase forms from spinach leaves. *Planta*, **153**, 351–361.

Streb, S. and Zeeman, S.C. (2014) Replacement of the endogenous starch debranching enzymes ISA1 and ISA2 of Arabidopsis with the rice orthologs reveals a degree of functional conservation during starch synthesis. *PloS One*, **9**, e92174.

Streb, S., Delatte, T., Umhang, M., Eicke, S., Martine, S., Didier, R. and Samuel, C.Z. (2008) Starch granule biosynthesis in Arabidopsisis abolished by removal of all debranching enzymes but restored by the subsequent removal of an endoamylase. *Plant Cell*, **20**, 3448–3466.

Subashinghe, R.M., Liu, F., Polack, U.C., Lee, E.A., Emes, M.J. and Tetlow, I.J. (2014) Multimeric states of starch phosphorylase determine protein-protein interactions with starch biosynthetic enzymes in amyloplasts. *Plant Physiol. Biochem.* **83**, 168–179.

Swallow, D.M. (2003) Genetic influences on carbohydrate digestion. *Nutr. Res. Rev.* **16**, 37–44.

Tetlow, I.J., Wait, R., Lu, Z., Akkasaeng, R., Bowsher, C.G., Esposito, S., Kosar-Hashemi, B. *et al*. (2004) Protein phosphorylation in amyloplasts regulates starch branching enzyme activity and protein-protein interactions. *Plant Cell*, **16**, 694–708.

The Potato Genome Sequencing Consortium (2011) Genome sequence and analysis of the tuber crop potato. *Nature*, **475**, 189–195.

Tuncel, A., Corbin, K.R., Ahn-Jarvis, J., Harris, S., Hawkins, E., Smedley, M.A., Harwood, W. *et al*. (2019) Cas9-mediated mutagenesis of potato starch-branching enzymes generates a range of tuber starch phenotypes. *Plant Biotechnol. J.* **17**, 2259–2271.

Uitdewilligen, J.G.A.M.L., Wolters, A.-M.A., D'hoop, B.B., Borm, T.J.A., Visser, R.G.F. and van Eck, H.J. (2013) A next-generation sequencing method for genotyping-by sequencing of highly heterozygous autotetraploid potato. *Plos One*, **8**, e62355.

Utsumi, Y., Utsumi, C., Sawada, T., Fujita, N. and Nakamura, Y. (2011) functional diversity of isoamylase oligomers: The ISA1 homo-oligomer is essential for amylopectin biosynthesis in rice endosperm. *Plant Physiol.* **156**, 61–77.

Veillet, F., Chauvin, L., Kermarrec, M.-P., Sevestre, F., Merrer, M., Terret, Z., Szydlowski, N. *et al*. (2019) The Solanum tuberosum GBSSI gene: a target for assessing gene and base editing in tetraploid potato. *Plant Cell Rep.* **38**, 1069–1080.

Wenqian, S., Zhou, Q., Yao, Y., Qui, X., Xie, K. and Yu, S. (2016) Identification of genomic regions and the isoamylase gene for reduced grain chalkiness in rice. *PloS One*, **10**, e0122013.

Wickramasinghe, H.A.M., Blennow, A. and Noda, T. (2009) Physico-chemical and degradative properties of in-planta re-structured potato starch. *Carbohydr. Polym.* **771**, 118–124.

Yang, R., Sun, C., Bai, J., Luo, Z., Shi, B., Zhang, J., Yan, W., and Piao, Z.. (2012) A putative gene sbe3-rs for resistant starch mutated from SBE3 for starch branching enzyme in rice (*Oryza sativa* L.). *PLoS One*, **7**, e43026.

Zeeman, S.C., Northrop, F., Smith, A.M. and apRees, T. (1998) A starch accumulating mutant of Arabidopsis thaliana deficient in a chloroplastic starch-hydrolysing enzyme. *Plant J.* **15**, 357–365.

Zhang, G., Cheng, Z., Zhang, X., Guo, X., Su, N., Jiang, L., Mao, L. *et al*. (2011) Double repression of soluble starch synthase genes SSIIa and SSIIIa in rice (*Oryza sativa* L.) uncovers interactive effects on the physicochemical properties of starch. *Genome*, **54**, 448–459.

Supporting information

Additional supporting information may be found online in the Supporting Information section at the end of the article.

Figure S1 Tuber morphology for control cultivars (Stabilo, Katinka, Oleva, 94-BVB-6, 93-CAL-3) and for IAm lines.
Table S1 Pedigree crossing. Parents with 100% *S. tuberosum genes* are indicted and *S. tuberosum* BC3 IAm lines having 6.25% *S. sandemanii* DNA including the 454 bp AFLP fragment are termed "tbr ex san".
Table S2 Tuber yield from field trials.
Table S3 Differentially expression between the IAm lines and the cultivars used for backcrossing.

